

Transient late gestation prenatal hypoxic insult results in functional deficits but not gross neuroanatomic deficits in mice

Ana G. Cristancho^{a, b, c}, Elyse C. Gadra^d, Ima M. Samba^a, Chenying Zhao^{e, f}, Minhui Ouyang^e, Sergey Magnitsky^e, Hao Huang^{e, g}, Angela N. Viaene^h, Stewart A. Anderson^{d, i}, and Eric D. Marsh^{a, b, c}

^a Division of Child Neurology, ^b Department of Pediatrics, Children's Hospital of Philadelphia, Philadelphia, PA, USA

^c Department of Neurology, Perelman School of Medicine at the University of Pennsylvania, Philadelphia, PA, USA

^d Department of Child and Adolescent Psychiatry and Behavioral Services, The Children's Hospital of Philadelphia, Philadelphia, PA, USA

^e Radiology Research, Children's Hospital of Philadelphia Research Institute, Philadelphia, PA, USA

^f Department of Bioengineering, School of Engineering and Applied Science, University of Pennsylvania, Philadelphia, PA, USA

^g Department of Radiology, Perelman School of Medicine, University of Pennsylvania, PA, USA

^h Department of Pathology, Children's Hospital of Philadelphia, Philadelphia, PA, USA and Perelman School of Medicine at the University of Pennsylvania, Philadelphia, PA, USA

ⁱ Department of Psychiatry, Perelman School of Medicine at the University of Pennsylvania, Philadelphia, PA, USA

Short Title: Deficits of transient prenatal hypoxia

Corresponding Author:

Ana G. Cristancho, MD, PhD
Abramson Research Center, Rm. 516g
Children's Hospital of Philadelphia,
3615 Civic Center Blvd.
Philadelphia, PA. 19104, USA
Tel: 267-426-6892
Email: cristanchoa@chop.edu

Keywords: prenatal hypoxia, animal model, behavior, imaging

Abstract

Intrauterine hypoxia is a common cause of brain injury in children with a wide spectrum of long-term neurodevelopmental sequelae even after milder injury that does not result in significant neuroanatomical injury. Published prenatal hypoxia models generally require many days of modest hypoxia or are invasive, difficult to replicate surgery to ligate the uterine artery. Postnatal models of neonatal hypoxic brain injury are not able to study the effects of antenatal risk factors that contribute to outcomes of hypoxia to the developing brain. In addition, the most common postnatal hypoxia models induce significant cell death and large focal neuroanatomic injury through unilateral ischemia, which is not a common pattern of injury in children. Large animal models suggest that brief transient prenatal hypoxia alone is sufficient to lead to significant functional impairment to the developing brain. Thus, to further understand the mechanisms underlying hypoxic injury to the developing brain, it is vital to develop murine models that are simple to reproduce and phenocopy the lack of neuroanatomic injury but significant functional injury seen in children affected by mild intrauterine hypoxia. Here we characterized the effect of late gestation (embryonic day 17.5) transient prenatal hypoxia on long-term anatomical and neurodevelopmental outcomes. Prenatal hypoxia induced hypoxia inducible factor 1 alpha in the fetal brain. There was no difference in gestational age at birth, litter size at birth, survival, fetal brain cell death, or long-term changes in gray or white matter between offspring after normoxia and hypoxia. However, there were several long-term functional consequences from prenatal hypoxia, including sex-dichotomous changes. Both males and females have abnormalities in repetitive behaviors, hindlimb strength, and decreased seizure threshold. Males demonstrated increased anxiety. Females have deficit in social interaction. Hypoxia did not result in motor or visual learning deficits. This work demonstrates that transient late gestation prenatal hypoxia is a simple, clinically-relevant paradigm for studying putative environmental and genetic modulators of the long-term effects of transient hypoxia on the developing brain.

29 Introduction

30 Acute hypoxic brain injury in neonates, known as hypoxic ischemic encephalopathy (HIE),
 31 accounts for millions of years lived with disability, including neurodevelopmental disabilities (NDDs),
 32 such as autism, and epilepsy [1, 2]. Children who are initially classified as having mild HIE, defined as
 33 minimal evidence of perinatal cell death by imaging and relatively normal neonatal physical exam,
 34 can still have adverse outcomes [3-7]. These children do not qualify for therapeutic hypothermia, the
 35 only specific intervention for moderate-severe HIE [8]. The incidence of HIE is disproportionately
 36 higher in children born in areas with limited prenatal care or access to therapies[9] so there is an
 37 urgent need for novel, widely available interventions.

38 To understand HIE, it is important to consider that *in utero* hypoxic injury differs from
 39 postnatal injury. The *in utero* environment is relatively hypoxic at baseline [10]. The required oxygen
 40 tension during fetal development is tightly regulated as evidenced by brain injury either from early
 41 exposure to relative hyperoxia in premature children or due to *in utero* hypoxia [11, 12]. While HIE is
 42 primarily an *in utero* injury, the most commonly used rodent model is a unilateral carotid ligation
 43 followed by hypoxia at day of life 7-10 (Vannucci Model) [13]. This model has provided many insights
 44 [14, 15] because neuroanatomically the rodent brain is considered “term” equivalent at post-natal
 45 day 7-10 [16]. However, injury in the Vannucci model is more focal with significant cell death that is
 46 most consistent with severe injury [13, 17] and this model cannot directly study the contributions of
 47 the maternal-placental unit to HIE severity [18, 19]. Additionally, functional networks do not
 48 correlate with neuroanatomy maturation in rodents [20]; mice do not have the respiratory or feeding
 49 dyscoordination at birth that is characteristic of children born before 34 weeks gestation [21], and
 50 they can walk by post-natal day 10, which is a developmental milestone acquired in infants at about
 51 a 12 months [20, 22]. Therefore, it is important to develop prenatal hypoxia models to understand
 52 key aspects of the pathophysiology of HIE as they affect development.

53 Mouse models of prenatal hypoxia exist, but they largely study the effects of chronic hypoxia
 54 by having dams live in mild hypoxia (~ 10% inspired oxygen) throughout gestation [23, 24] or are
 55 technically challenging (late gestation uterine artery ligation) [25]. There have been a few studies of
 56 transient prenatal hypoxia in rodents [26, 27], but most of our understanding of brief, mild insults is
 57 from large animal studies. In sheep, transient prenatal hypoxia leads to long-term structural and
 58 functional injury despite the absence of cell death, including deficits in neuron dendritic complexity
 59 and action potential propagation [28, 29].

60 To complement existing models and determine if transient hypoxia has similar findings as
 61 seen in large animal studies, here we characterize a simplified model of transient prenatal hypoxia. In

particular, we focus on early and late neuroanatomic injury using clinically analogous pathology and neuroimaging measures as well as wide battery of behavioral studies to determine if this model correlates to mild hypoxic injury seen in children.

Materials and Methods

Animals

Male and female C57Bl/6 mice were purchased from Charles River Laboratories (Wilmington, MA). Timed matings were used to ensure consistent timing of prenatal hypoxia exposures. Mice were maintained at the Children's Hospital of Philadelphia Animal Facility at a 12-hour light, 12-hour dark cycle (0615-1815 h) and ad libitum access to water and diet mouse food 5015 (LabDiet, St. Louis, MO). Offspring exposed to prenatal normoxia or hypoxia were periodically weighed by experimenters blinded to exposure. Animals were group housed for postnatal experiments. Male and female gonadectomized CD1 mice for Social Interaction were acquired from Charles River Laboratories. The Institutional Animal Care and Use Committee of the Children's Hospital of Philadelphia approved all experiments.

Prenatal hypoxia

Pregnant females were placed in a controlled oxygen chamber (BioSpherix Ltd., Parish, NY) at embryonic day 17.5 (E17.5). Mice were acclimated to the chamber for 1-2 minutes at 21% oxygen. For hypoxic exposures, oxygen concentration was decreased to 5% oxygen over 30 minutes and maintained at 5% oxygen for duration of experiment (2, 4, 6, or 8 hours). For normoxic control exposures, pregnant mice were placed in the same controlled oxygen chamber for 8 hours. Dams in both groups were provided free access to food and hydrogel for hydration throughout the time in chamber. For locomotion, pregnant mice (normoxia n=4, hypoxia n=4) were videotaped during first 90 minutes in the chamber and cumulative distance the mouse moved in chamber was quantified with ANY-maze software (Stoelting Co., Wood Dale, IL, USA). Except for protein and RNA studies, after hypoxia, pregnant dams were monitored for recovery and demonstrated normal locomotion within 10 minutes of end of exposure. All survival studies were performed after 8 hours of prenatal hypoxia. Pregnant dams from normoxia and hypoxia were assessed twice per day until delivery to determine gestational age at birth and number of pups per litter at birth.

RNA isolation and quantitative PCR

Messenger RNA (mRNA) was isolated from flash frozen samples using RNeasy Lipid Tissue Mini Kit (QIAGEN, Venlo, Netherlands). RNA was isolated with DNase to avoid contamination. Individual samples shown were isolated from n =11-12 fetal brains/condition in 3 separate litters/condition. RNA was converted to cDNA with High-Capacity cDNA Reverse Transcription Kit (Applied Biosystems, Foster City, CA). Quantitative PCR on Quant Studio 12K Flex (Applied Biosystems, Foster City, CA) was used to quantitate mRNA levels with Taqman of 18s as a housekeeping gene (Mm03928990_g1, Thermo Fisher Scientific, Waltham, MA) and the HIF1 α target gene, *Vegfa* (Mm00437306_m1, Thermo Fisher Scientific, Waltham, MA). *Vegfa* levels were normalized to 18S levels in each sample. To normalize between different plates, average of the normoxic condition, were standardized to 1 and all other samples on that plate were multiplied by the sample standardization factor.

Maternal nestlet

Ability for pregnant dams after normoxia or hypoxia to form a nest was used as a proxy for the ability to form a nurturing environment. A 5-point scale was utilized as previously described, with a score of 5 being an intact nest [30]. In brief, after 8 hours in oxygen chamber in normoxia or hypoxia, pregnant dams were placed in new cage with intact cotton squares and no other environment enrichment cage. They were placed in standard holding room overnight. The following morning an experimenter obtained an overhead picture of the cage with minimal disruption. A blinded experimenter scored the pictures.

Histology

Fetal brains were harvested 24 hours after exposure and placed in 4% paraformaldehyde. Fixed brains were placed in the coronal plane, processed and paraffin-embedded and then cut by the CHOP Pathology Core into 5 μ M unstained slides. Every fifth slide was stained with hematoxylin and eosin and examined to identify brain regions of interest. Pyknotic nuclei in cortex, basal ganglia, and white matter were counted by neuropathologist (A.N.V.) who was blinded to condition (n = 3 condition).

Ex vivo MRI

High resolution diffusion tensor imaging (DTI), one type of MRI, is an effective noninvasive imaging tool to delineate neuroanatomy [31-33]. Here we used high resolution DTI (0.1×0.1×0.1mm) with MR scanner of high magnetic strength to examine the morphological and microstructural changes in mice with hypoxia.

MRI data acquisition

The MRI data was acquired on a Bruker 9.4T vertical bore scanner. A volume coil with inner diameter of 15mm was used as RF transmitter and receiver. A 3D high-resolution, multi-shot echo planar imaging (EPI) sequence with eight shots was used to acquire diffusion-weighted images (DWIs). The parameters for DWIs were as follows: field of view=25.6×12.8×10.0mm; voxel size=0.1×0.1×0.1mm; echo time=26ms; repetition time=1250ms; 6 or 30 independent diffusion-weighted directions with a b value of 1500 s/mm² and five additional images without diffusion gradients; two averages.

Diffusion tensor fitting

Diffusion tensor was fitted in DTIStudio (<http://www.MRlstudio.org>) [34]. After the diagonalization of tensor to obtain three eigenvalues ($\lambda_{(1-3)}$) and eigenvectors ($v_{(1-3)}$), mean diffusivity (MD) was calculated as the mean of three eigenvalues ($\lambda_{(1-3)}$). Fractional anisotropy (FA) was calculated as follows.

$$FA = \frac{\sqrt{(\lambda_1 - \lambda_2)^2 + (\lambda_1 - \lambda_3)^2 + (\lambda_2 - \lambda_3)^2}}{\sqrt{2}\sqrt{\lambda_1^2 + \lambda_2^2 + \lambda_3^2}}$$

Regions of interest (ROIs) delineation, and measurements of volume and thickness

The ROIs, including ventricles, were manually placed on the averaged b0 map or MD map by referencing known stereotactic reference atlas [35] in ROIEditor (<http://www.MRlstudio.org>). For genu and splenium of the corpus callosum, the ROIs of consistent size were drawn on seven slices around mid-sagittal slice of the brain. The volume of the ventricles was calculated as the number of voxels in the ROI times the voxel size. The thickness of anterior cingulate cortex was measured in the mid-sagittal region. Volume and thickness measurements were calculated in Matlab (Mathworks, Inc., Natick, MA, USA).

153

154 *Behavior*

155 Behavior studies following published protocols were performed sequentially starting at 3
156 months old in the order listed below for all animals [36-42] Any modifications are listed below. Three
157 separate cohorts consisting of a total of 5 normoxic litters and 4 hypoxic litters were used.
158 Composition of experimental groups consisted of normoxic male = 16, hypoxic male = 10, normoxic
159 female = 22, hypoxic female = 13.

160 All testing except for grip strength was performed between 0700 h to 1300 h. Grip strength
161 was performed from 1400 h to 1600 h. All animals were given at least 1 day and up to 7 days of rest
162 between behavior paradigms to minimize carrying effect between studies. Weight was monitored
163 before each test to ensure there was weight loss consistent with poor health or significant fatigue
164 between experimental days. No mice were removed from these experiments for outliers. Animals
165 were not acclimated to handling before Elevated zero maze or Open field, but were subsequently
166 handled daily between experimental days for 5 minutes per cage. Mice were acclimated to
167 experimental room at least 30 minutes prior to protocol. Equipment apparatus was cleaned with
168 cleaning wipes between mice (PDI Sani-Cloth Plus germicidal disposable cloth). ANY-maze software
169 (Stoelting Co., Wood Dale, IL, USA) was used to video-record and score Elevated zero maze, Open
170 field, Social interaction, and Morris water maze.

171

172 *Elevated zero maze*

173 Elevated zero maze was modified from previous description [42]. In brief, annular 60 cm
174 diameter beige apparatus was elevated 50 cm above the ground, with care to ensure it was level.
175 Two opposing quadrants were “open” and the other two opposing quadrants were “closed” with 16
176 cm opaque walls but no cover. Experimenter was hidden from the apparatus by black drape
177 surrounding the apparatus. Illumination was provided overhead with open arms approximately 150-
178 200 lumens/m² and closed arms at 50 lumens/m². Animals were placed in the center of a closed arm
179 and allowed to roam the apparatus freely for 5 minutes. In addition to time in open arm, head
180 entries into the open arms and time freezing (immobile at least 1 sec) were detected by ANY-Maze.

181

182 *Open field*

183 Open field was modified from described protocol [41]. In brief, A 53 × 53 cm white plastic box
184 with 22-cm high walls and no top. Illumination was from overhead fluorescent lights in the 150-200

lumens/m² range. Experimenter was visually separated from animals in apparatus by black drape. Each mouse was placed in the center of the box and allowed to roam freely in the box for 15 min. ANY-maze scored a mouse to be in the periphery if it was within 13 cm of the wall of the box and otherwise they were considered to be in the center of the box. The distance traveled during the test in the entire apparatus was also measured.

Marble burying

Marble burying was modified from previous studies [36, 38]. A white 41.9 cm x 33.7 cm x 22.5 cm box was filled with 5 cm of fresh bedding. Twenty-four marbles were arranged in a 4 x 6 grid 5 cm apart. Up to 6 mice were tested at the same time so further barriers were placed between the boxes. Illumination was provided by overhead lights with range of 130-150 lumens/m² at each box. Each mouse was placed in the center of the box for 30 minutes and allowed to roam freely. Pictures were taken before animals were placed of each chamber and then at the end of the 30 minutes. Two blinded reviewers examined images to determine whether marbles were buried greater than 2/3rd into the bedding. Average from the two reviewers of marbles buried for each mouse is reported.

Short term nestlet

Short term nestlet experiment was modified from previous study [38]. Animals were placed in a clean cage with 1 cm of fresh bedding. A pre-cut nestlet with all rough edges removed was weighed and placed in the center of the cage. Each mouse was placed in the center of the chamber away from the experimenter and cage lid was placed on top. The mouse was allowed to roam freely in the chamber for 30 minutes. As multiple animals were in the cages at the same time, barriers were placed to visually separate the animals. At the end of the 30 minutes, the animals were removed. Nestlets were removed from the cage and allowed to dry overnight. A blinded experimenter removed any pieces of easily removable nestlet and weighed them after > 24 hours of drying. Change in nestlet weight was calculated by subtracting from the pre-experiment nestlet weight.

Rotarod

Mice were tested on a Rotarod from Ugo Basile (Model 47650, Comerio, Italy) as previously published [40]. The mice were tested in groups, 5 at a time for 5 min trials with 3 trials per day for 4 days. The Rotarod was used in acceleration mode. The first 2 days, speed increased from 4 rpm up to

40 rpm. The last 2 days, speed increased from 8 rpm to 80 rpm. The speed at falling, grappling the rod without walking for 4 consecutive cycles, or end of 5 minutes for each mouse was recorded as the end of each trial. Between trials the mice were placed back into individual containers and at the end of the last trial placed back in home cages. Intertrial time was 15-20 minutes.

Social interaction

Social interaction and choice were tested as per previously described [41]. White three chamber apparatus was filled with 1-2 cm of fresh bedding. The experiment was performed in red light without fluorescence to resemble night time environment when mice are most likely to interact. For habituation stage, the experimental mouse was placed for 10 min in apparatus with an empty clear tube with holes was placed in the center of the left and right chambers. The experimental mouse was then placed in a temporary holding chamber prior to the next stage. For the novel mouse/object stage, a sex matched gonadectomized mouse was placed in the tube on the left. In the tube on the right, a novel object was placed. The experimental animal was then returned to the apparatus for 5 min. In addition to time in chamber, animals were considering to be “sniffing” the tube if the head was within 2 cm of the tube by ANY-maze.

Grip strength

The grip strength of the mice was tested using a grip strength meter (Model 080312-3 Columbus Instruments, Columbus, OH, USA) as previously published in the Marsh lab [41]. In brief, each mouse was tested in 6 consecutive trials; 3 were for forelimbs, and 3 for hindlimbs. Each trial was recorded, and the average for each mouse for forelimb and hindlimb trials is reported.

Morris water maze

Morris water maze was performed in a 128 cm round plastic tube filled with room temperature water (approximately 21°C) as previously published [37, 41]. A platform was submerged 0.5 cm below water surface. Non-toxic white tempera paint was used to opacify the water so the platform could not be seen from the ledge. Testing was performed in 3 phases: visual acuity trials, place trials, and probe testing. For both trial phases, in each trial a mouse was allowed to swim for up to 60 sec to find the platform or was led there at the end of the 60 sec. Once on the platform, the mouse was maintained on the platform for 15 seconds prior to being dried and placed under a heat

lamp for the following trial if having difficulty with drying its coat. There were 4 trials per day. The visual acuity of each mouse was tested for 2 days by placing a flag that could be seen above the platform. For each trial, the platform with flag and the location of the mouse was placed in was changed. A mouse was considered to have normal vision if by the 2nd day it was able to find the platform at least 50% of the trials before 60 seconds. All mice were deemed to have normal vision. Place trials were then performed for 5 days. Flag was removed from platform and the platform was completely submerged in the southwest quadrant. Visual cues were placed in the north, south, east, and west markers of the tub. For each trial, a mouse was placed in a different location of the tub. Time to platform and path efficiency were measured in ANY-Maze and average of these measures for all the trials for each day was reported. For probe testing, platform was removed from the pool. One hour after last place trial, each mouse was placed in the northeast quadrant and allowed to swim freely for 60 seconds to assess short term memory. Time spent swimming the in southwest quadrant, where the platform had been located, was measured. Twenty-four hours after the last place trial, probe test was repeated to assess long-term memory.

Flurothyl seizure threshold

Flurothyl (bis-2,2,2-trifluoroethyl ether, Sigma, St. Louis, MO) testing was modified from procedure previously described [43, 44]. In brief, 5 to 6 month old mice were place on a platform in a 1.7 L rubber sealed glass chamber (Ikea, Älmhult, Sweden) containing a small amount of the carbon dioxide scavenger, soda lime (Sigma). Flurothyl was infused with syringe pump at a rate of 6 mL/hour until the first generalized tonic-clonic seizure (GTC) was observed. The experimenter was blinded to condition during the experiments. Animals were videotaped throughout the experiment. Two blinded scorers used a modified Racine scale to define a generalized tonic-clonic seizure [15].

Statistical analysis

All animal experiments were performed with experimenter blinded to exposure condition. The majority of the data is presented using truncated violin plots with individual mice plotted superimposed on top to display frequency distribution (GraphPad, San Diego, CA). Data are grouped by hypoxia and sex. Markings on violin plots are as follows: center dashed line is the median value and lighter lines demonstrate quartiles.

For statistics, GraphPad and R-studio were used. Area under the curve was determined for locomotion of pregnant dams and unpaired t-test was calculated. Mann-Whitney test was used to

compare normoxia and hypoxia maternal nestlet shredding, gestational age, litter size, and MRI studies. Log-rank test was utilized for survival. For RNA, One-Way Nested ANOVA was used in Graphpad. For all other studies, R was used for statistics. Mixed models with generalized estimating equations in geepack package in R was utilized for majority of comparisons [45]. Linear mixed-effects models in lme4 package in R was used for experiments requiring analysis of daily repeated measures (weights, Rotarod, Morris Water Maze) [46]. Cohort was used as a random effect. Independent variables for all models included prenatal hypoxia exposure, sex, birth gestational age, and litter size at birth. Statistical significant displayed for hypoxia, sex, and interaction between hypoxia and sex as hypoxia has been shown to have sex-dichotomous effects [47, 48]. Statistical significance was set at * $p < 0.05$, ** $p < 0.01$, and *** $p < 0.001$ with “#” symbol used for sex-specific effects. A Benjamini-Hochberg correction was used for all p-values from mixed model analyses. Statistical subanalysis for differences for hypoxia based on sex were only performed if hypoxia or interaction between sex and hypoxia had an adjusted $p < 0.15$ to determine if there were more subtle effects unique to each sex or by condition based on the day. Shapiro-Wilk test was used to determine the normality of the distribution within each test. If the distribution was normal, the mean and standard deviation are reported. If the distribution was not normal, the median and interquartile range (IQR) is reported.

Results

Prenatal hypoxia induces the canonical hypoxic response in the fetal brain

First, we performed a time course to determine the duration of prenatal hypoxia that was required to induce a reproducible hypoxic molecular response in the fetal brain. The transcription factor hypoxia inducible factor 1 alpha (HIF1 α) and its canonical target, vascular endothelial growth factor A (*Vegfa*), are established molecular markers of the hypoxic response [49]. HIF1 α protein is stabilized by the intrinsically hypoxic in utero environment [50] but it can be induced further over time by prenatal hypoxia (**Fig. 1A & 1B**). *Vegfa* mRNA levels also increased with prenatal hypoxia (**Fig. 1C**). While the peak of increase for both protein and mRNA was at 4 hours of hypoxia, there was decreased variability in samples after 8 hours of hypoxia, particularly in *Vegfa* levels. Thus, 8 hours of hypoxia was used for all further experiments.

Maternal and offspring survival and health were unaffected by prenatal hypoxia

Pregnant mice demonstrated a decrease in locomotor activity during hypoxic exposure once oxygen was less than 10% FiO₂, approximately 20 minutes after start of the hypoxia protocol (**Fig.**

2A). They survived 8 hours of hypoxia and rapidly recovered during brief observation. Given pregnant mice locomotion was affected by hypoxia, we tested whether their ability to rear offspring after hypoxic exposure may be grossly altered. After normoxia or hypoxia, we placed the pregnant mice in a new clean cage with an intact nestlet square and compared the difference in making a nest as a proxy for creating a nurturing environment. Sixteen hours after exposure, almost all mice of both conditions made normal nests (**Fig. 2B**).

Offspring health after normoxia and hypoxia was assessed by litter size at birth, birth gestational age, survival, and weight. There was no statistical difference in litter size at birth (**Fig. 2C**) or birth gestational age (**Fig. 2D**). In addition, there was no difference in survival of mice through the first 90 days of life (**Fig. 2E**). Together these results suggest that maternal dams can tolerate and appropriately rear offspring after prenatal hypoxia and that there is not a severe, life threatening phenotype from prenatal hypoxia on the offspring.

Prenatal hypoxia does not increase cell death in the fetal brain

In the Vannucci model there has been efforts to determine the kinetics of apoptosis after injury where apoptosis peaks at 24-28 hours after injury in the co [51]. Based on this work, we isolated the fetal brain 24 hours after exposure to hypoxia and normoxia (at E18.5), prior to being born to avoid any confounding effects from birth. A neuropathologist blinded to the exposure condition then counted pyknotic nuclei (**Fig 3A**) in the cortex, basal ganglia, and white matter, three regions that can have significant cell death in children with acute perinatal hypoxic injury [14]. There was no increase in pyknotic nuclei in any region of the brain analyzed (**Fig. 3B-3D**).

Prenatal hypoxia does not lead to long-term neuroanatomical deficits

To determine if there were long-term neuroanatomic deficits, we performed *ex vivo MRI* in adult animals that were exposed to normoxia or hypoxia prenatally. Lateral ventricle volume was measured and demonstrated a substantial variability between hypoxic animals (**Fig. 4A**), but overall there was no significant increase in lateral ventricle size (**Fig. 4B**) or differences in cortical thickness of the anterior cingulate (**Fig. 4C & D**). Similarly, DTI derived FA measurement of the corpus callosum, an index of the extent of fiber alignment and myelination, demonstrated no difference between groups in white matter microstructure of the genu or splenium of the corpus callosum (**Fig. 4C, E & F**).

Prenatal hypoxia leads to multiple behavior deficits in adult animals

Multiple behavioral domains were tested to determine if prenatal hypoxia leads to long term deficits that are consistent with differences seen in children with prenatal hypoxic injury. Results could be divided into three categories – deficits in males and females, sex-dichotomous deficits, and no deficits. The most striking difference between normoxic and hypoxic animals was in seizure threshold. Children with moderate to severe HIE have an increased risk of developing epilepsy after the acute period [52, 4]. While we did not observe any spontaneous seizures or see sudden death that would be consistent with uncontrolled epilepsy, we sought to determine if hypoxic animals had a decrease in seizure threshold through flurothyl seizure threshold testing [43]. We determined that hypoxic mice had a decreased seizure threshold (mean/SD normoxic male = 229.3 s +/- 53.5, hypoxia male = 200.0 s +/- 30.3, normoxic female = 211.8 s +/- 47.9, hypoxic female = 182.6 s +/- 27.7) (**Fig. 5A**). This data suggest that prenatal hypoxia may predispose animals to subtle network deficits consistent with decreased seizure threshold.

We performed grip strength to determine whether hypoxic mice had long-term motor deficits [53]. There was a difference at baseline between male and female animals, but there was no decrease in forelimb grip strength due to prenatal hypoxia (mean/SD normoxic male = 0.044 kg of force +/- 0.016, hypoxic male = 0.045 kg of force +/- 0.013, normoxic female = 0.037 kg of force +/- 0.012, hypoxic female = 0.039 kg of force +/- 0.009) (**Fig. 5B**). By contrast, hindlimbs did demonstrate a difference between normoxic and hypoxic animals (mean/SD normoxic male = 0.020 kg of force +/- 0.006, hypoxic male = 0.020 kg of force +/- 0.007, normoxic female = 0.026 kg of force +/- 0.009, hypoxic female = 0.021 kg of force +/- 0.008) (**Fig. 5C**), suggesting mild motor impairment after prenatal hypoxia.

We also determined if there were any differences in compulsive and repetitive behaviors [36, 38]. Increased marble burying has been associated with an obsessive compulsive related phenotype [38], but decrease in marble burying has been seen in genetic models of autism, suggesting decrease in this typical behavior is also pathogenic [54, 55]. Hypoxic animals, particularly females, had a decrease in marbles buried (mean/SD normoxic male = 10.34 n +/- 5.99, hypoxic male = 6.30 n +/- 5.32, normoxic female = 9.55 n +/- 4.45, hypoxic female = 3.85 n +/- 2.48) (**Fig. 5D**). Consistent with decreased repetitive behaviors in Marble burying, hypoxic mice demonstrated significant decrease in a short-term nestlet shredding study, but in this assay the deficit was more prominent in males (median/IQR normoxic male = -0.05 g /0.20, hypoxic male = -0.10 g/0.20, normoxic female = -0.10 g/0.38., hypoxic female = -0.1 g +/- 0.25) (**Fig. 5E**).

Prenatal hypoxia leads to some sex-dichotomous behavior differences in anxiety and social interaction

Anxiety seemed more prevalent in hypoxic males using two different assays. Elevated zero maze is considered a strong anxiogenic stimulus for animals, where increased anxiety is associated with decreased time in the open arms of the apparatus [56]. Hypoxic male animals spent less time in the open arms than normoxic male animals and there was no effect on females (mean/SD normoxic male = 144.7 s +/- 51.8, hypoxia male = 112.0 s +/- 33.9, normoxic female = 139.0 s +/- 53.7, hypoxic female = 144.9 s +/- 40.8) (**Fig. 6A**). We then aimed to determine if this phenotype was confirmed Open field, another well-established assay for anxiety where increased anxiety is associated with decrease time in the center of the apparatus [56]. Here we observed that hypoxic male mice spent less time in the center of the field than normoxic male mice (median/IQR normoxic male = 151.8 s/128.8, hypoxic male = 127.6 s/105.3) (**Fig 6B**). Notably, female mice spend less time than male mice in the center in general and there was no added affect by hypoxia (normoxic female = 86.3 s/69.0., hypoxic female = 84.5 s/104.7).

Hypoxic insults can be associated with social deficits like autism [57], so we performed three chamber social interaction testing. In the initial stage of this test, we demonstrated that mice did not have any preference for the left or right side of the chamber (**Fig. 6C & D**). Hypoxic males did tend to spend more time in the center chamber than the normoxic counterparts consistent with lack of exploration seen in the anxiety assays. In the second stage, a novel mouse was placed in a cup in the left side of the chamber and a novel object was placed on the right side of the chamber. As expected, normoxic males and females demonstrated a preference for the novel mouse compared to the novel object (**Fig. 6E & F**). Hypoxic male animals demonstrated a similar increase in preference for the novel mouse (**Fig. 6E**). However, hypoxic female mice did not have as strong of a preference for the novel mouse (**Fig. 6F**), suggesting a decrease in social interaction only in female animals.

Prenatal hypoxia does not lead to deficits in learning or memory

To determine whether prenatal hypoxia led to more significant deficits in learning or memory, we tested motor learning and visual spatial learning and memory. In Rotarod testing for motor learning and coordination [40], there was no difference between hypoxia and normoxia (**Fig. 7A**).

Morris water maze was used to test for deficits in learning and memory [37] to recapitulate the learning disabilities found in children with more severe HIE [4, 58]. Place trials demonstrated there was no difference between normoxic and hypoxic mice in time to platform (**Fig. 7B**). Probe testing in Morris water maze was used to determine if there were any differences in memory. Prenatal hypoxia did not predispose mice of either sex to short or longer term memory deficits (**Fig.**

7C & D). Together, this data suggests that prenatal hypoxia does not predispose animals to significant cognitive deficits.

Discussion/Conclusion

In this study, we have demonstrated that this novel and simple prenatal hypoxia protocol recapitulates several key features seen in children born after mild HIE, including deficits in anxiety [59], motor function [60], and susceptibility to seizures [4, 58]. These functional deficits occur in the absence of long term structural deficits, which is also consistent with lack of gross anatomic deficits in children with mild HIE [4, 61]. Together these data suggest that this model of transient prenatal hypoxia is most similar to mild neurodevelopmental deficits after mild HIE, a clinically important group of patients. Mild impairment outcomes account for about 25% of children with perinatal hypoxia even in the setting of therapeutic postnatal hypothermia [58]. About half of the children with mild HIE, including children with normal or mild neonatal MRI findings, will have functional impairment 9-10 years later [4]. Therefore, the significance of this model stems from its relationship to the clinically-relevant context of HIE it was established to model.

This model offers a few specific strengths for studying the mechanisms driving hypoxic brain injury. First, HIE is generally a prenatal insult so this model of antenatal hypoxic injury is an important addition to the complement of postnatal models because it allows future study understanding the physiology of in utero insult. The fetal environment is intrinsically hypoxic at baseline [50, 26], so worsening in utero hypoxia in this model is likely compensated for differently than hypoxia in the ex utero environment. Indeed, HIF1 α in neural cells is required for normal brain development [62], indicating the importance of hypoxia during brain development. In this model of prenatal hypoxia, HIF1 α protein levels increase within the first 4 hours of hypoxia, but then appears to decrease. This decrease in HIF1 α at 8 hours of hypoxia, suggests that in utero there may be an initial capacity to compensate for hypoxia that is lost over time. The fluctuation of HIF1 α levels during different duration of hypoxia may someday be found to have clinical relevance since the duration of in utero hypoxic injury prior to HIE can be elusive because by definition relies on recognition of the hypoxic event by mother or providers [14, 63]. Therefore, it is feasible that there is significant period of time with decreased oxygenation in utero delivery prior to recognition for urgent delivery. Furthermore, antenatal risk factors for chronic prenatal hypoxic injury, such as excessive weight gain during pregnancy, are risk factors for worse outcomes from HIE [64]. This possible detrimental effect of prenatal chronic hypoxia on acute hypoxic neonatal injury is in sharp contrast to postnatal adult stroke studies where hypoxic preconditioning is protective of acute and long-term

injury [65]. The epidemiological link between chronic hypoxia conditions in utero and acute hypoxic in utero injury warrants further study and this model is poised to study these acute-on-chronic interactions.

Second, this model offers the opportunity to study the effects of hypoxia on diffuse brain injury. This model does not include a true “ischemic” component, such as is seen in the most commonly used Vannucci model [13]. Accordingly, it lacks gross neuronal injury that has been associated with the most severe cases of children with HIE [17]. However, models in various different organisms have demonstrated that transient global hypoxia is capable of producing significant neurological sequelae [66, 48]. Likely due to the absence of significant neuronal death, there is a wide variability in the phenotypes of prenatal hypoxic mice; overall with more nuanced findings. This prenatal model may provide an attractive platform for studying the genetic factors that exacerbate the mild phenotype; it may provide mechanistic insight into why 40% of patients have moderate to severe disability after HIE by determining if there are pathways that may increase cell death and worsened behavior deficits in the setting of this mild prenatal hypoxia model.

Third, this model allows for studying the effects of hypoxia on development of functional networks after hypoxic injury. The majority of models of acute HIE are performed at day 7-10 of life in mice because, neuroanatomically, the rodent brain at birth is approximately equivalent to a 23-30 week gestation human brain and is considered “term” equivalent at post-natal day 7-10 [16]. However, functional networks in rodents are not correlated with neuroanatomical development [20]. Mice do not have respiratory distress or feeding dyscoordination at birth that is characteristic of children born at less than 34 weeks gestation [21]. Furthermore, mice acquire the ability to crawl within a few days of life and are generally capable of walking by post-natal day 10, which is generally a developmental milestone acquired in a 12 month old infant [20]. Thus, for future directions this model of prenatal hypoxia is well-suited to study the effect of hypoxia on clinically-relevant networks that are still developing in the term human brain, through behavior and electrophysiology. Additionally, preterm HIE is an understudied, but likely important clinical modulator, of neurodevelopmental outcomes in preterm infants [67]. While white matter is diffusely affected in premature infants and we did not see differences in the corpus callosum, lack of abnormality in the corpus callosum does not rule out more subtle effects in white matter development [68].

Lastly, this model may help study the effects of sex on outcomes from prenatal hypoxia. Clinical studies of long-term outcomes of HIE are underpowered to determine sex-related differences in long-term outcomes [69, 58] but have been suspected since there are sex differences from other causes of perinatal brain injury [70]. Sex differences have been observed in other models of hypoxia and hypoxic-ischemic injury [71, 70, 72, 48]. It is not clear if there are consistent sex-dichotomies in

anxiety or autism in patients. In particular, it is also not clear if differences in females in social interactions in this mouse model has a true clinical correlate since males are typically most affected by autism in general [73]. Future studies in this model will be centered on understanding the relationship between observed anatomical differences and behavioral differences, particularly trying to determine the mechanisms underlying the observed sex-dichotomy.

In conclusion, here we present a simplified, easy to reproduce model prenatal hypoxic injury model that phenocopies many of the functional deficits consistent with findings in children with mild HIE. This work provides a novel model to study the effect of this common prenatal stressor in a biologically and clinically significant context. We expect these results will provide a novel platform to study the effects of antenatal risk factors and genetic modifiers on transient hypoxia during brain development, the effects of hypoxia on early postnatal developmental circuits, and sex-dependent effects that may be leveraged for treating children at risk for long-term neurodevelopmental abnormalities from perinatal hypoxia injury. With comparative studies amongst models of prenatal and postnatal injury we can better understand the full spectrum of relevant disease from hypoxia to the developing brain and determine opportunities for novel interventions.

Acknowledgement

We thank the Small Animal Imaging Facility at the Research Institute of the Children's Hospital of Philadelphia (CHOP), the CHOP Pathology Core, and the Neurobehavior Testing Core, and EEG/Epilepsy core at UPenn and IDDRC at CHOP/Penn [Grant: U54 HD086984] for assistance. We thank Dr. Rui Xiao in the Department of Biostatistics at UPenn for her advice on statistical analysis. We thank Brenna Daugherty for initial studies monitoring pregnant mouse locomotion. We are grateful to Daniel Licht and the Wolfson family for providing the Biospherix oxygen chambers. We are grateful to Dr. Michal Elovitz and members of the Marsh and Anderson labs for numerous insightful discussions conversations regarding the data in this manuscript.

Statement of Ethics

Studies involving animals were approved by the Institutional Animal Care and Use Committee (IACUC) at the Children's Hospital of Philadelphia.

Conflict of Interest Statement

The authors have no conflicts of interest to declare.

510

511 **Funding Sources**

512 This work was supported by the National Institutes of Health [Grant: 5K12HD043245-18,
513 R01MH092535, R01MH092535-S1 and U54HD086984], and institutional grants from the Children's
514 Hospital of Philadelphia, including Neurology Black Tie Tailgate Fund, Foerderer Grant, and K-
515 readiness Pilot award.

References

1. Lee AC, Kozuki N, Blencowe H, Vos T, Bahalim A, Darmstadt GL, et al. Intrapartum-related neonatal encephalopathy incidence and impairment at regional and global levels for 2010 with trends from 1990. *Pediatr Res*. 2013 Dec;74 Suppl 1(SUPPL. 1):50-72.
2. Stanaway JD, Afshin A, Gakidou E, Lim SS, Abate D, Abate KH, et al. Global, regional, and national comparative risk assessment of 84 behavioural, environmental and occupational, and metabolic risks or clusters of risks for 195 countries and territories, 1990–2017: a systematic analysis for the Global Burden of Disease Study 2017. *The Lancet*. 2018;392(10159):1923-94.
3. de Haan M, Wyatt JS, Roth S, Vargha-Khadem F, Gadian D, Mishkin M. Brain and cognitive-behavioural development after asphyxia at term birth. *Dev Sci*. 2006 Jul;9(4):350-8.
4. van Kooij BJ, van Handel M, Nievelstein RA, Groenendaal F, Jongmans MJ, de Vries LS. Serial MRI and neurodevelopmental outcome in 9- to 10-year-old children with neonatal encephalopathy. *J Pediatr*. 2010 Aug;157(2):221-27 e2.
5. Eunson P. The long-term health, social, and financial burden of hypoxic-ischaemic encephalopathy. *Dev Med Child Neurol*. 2015 Apr;57 Suppl 3:48-50.
6. Reiss J, Sinha M, Gold J, Bykowski J, Lawrence SM. Outcomes of Infants with Mild Hypoxic Ischemic Encephalopathy Who Did Not Receive Therapeutic Hypothermia. *Biomed Hub*. 2019 Sep-Dec;4(3):1-9.
7. Schreglmann M, Ground A, Vollmer B, Johnson MJ. Systematic review: long-term cognitive and behavioural outcomes of neonatal hypoxic-ischaemic encephalopathy in children without cerebral palsy. *Acta Paediatr*. 2020 Jan;109(1):20-30.
8. Ahearne CE, Boylan GB, Murray DM. Short and long term prognosis in perinatal asphyxia: An update. *World J Clin Pediatr*. 2016 Feb 8;5(1):67-74.
9. Chin EM, Jayakumar S, Ramos E, Gerner G, Soares BP, Cristofalo E, et al. Preschool Language Outcomes following Perinatal Hypoxic-Ischemic Encephalopathy in the Age of Therapeutic Hypothermia. *Dev Neurosci*. 2019 Jun 5:1-11.
10. Hutter D, Kingdom J, Jaeggi E. Causes and mechanisms of intrauterine hypoxia and its impact on the fetal cardiovascular system: a review. *Int J Pediatr*. 2010;2010:401323.
11. Jauniaux E, Watson AL, Hempstock J, Bao YP, Skepper JN, Burton GJ. Onset of maternal arterial blood flow and placental oxidative stress. A possible factor in human early pregnancy failure. *Am J Pathol*. 2000 Dec;157(6):2111-22.
12. Panfoli I, Candiano G, Malova M, De Angelis L, Cardiello V, Buonocore G, et al. Oxidative Stress as a Primary Risk Factor for Brain Damage in Preterm Newborns. *Front Pediatr*. 2018;6:369.
13. Rice JE, 3rd, Vannucci RC, Brierley JB. The influence of immaturity on hypoxic-ischemic brain damage in the rat. *Ann Neurol*. 1981 Feb;9(2):131-41.
14. Ferriero DM. Neonatal brain injury. *N Engl J Med*. 2004 Nov 4;351(19):1985-95.
15. Sun H, Juul HM, Jensen FE. Models of hypoxia and ischemia-induced seizures. *J Neurosci Methods*. 2016 Feb 15;260:252-60.
16. Semple BD, Blomgren K, Gimlin K, Ferriero DM, Noble-Haeusslein LJ. Brain development in rodents and humans: Identifying benchmarks of maturation and vulnerability to injury across species. *Pergamon*; 2013. p. 1-16.
17. Northington FJ, Chavez-Valdez R, Martin LJ. Neuronal cell death in neonatal hypoxia-ischemia. *Ann Neurol*. 2011 May;69(5):743-58.
18. Badawi N, Kurinczuk JJ, Keogh JM, Alessandri LM, O'Sullivan F, Burton PR, et al. Antepartum risk factors for newborn encephalopathy: the Western Australian case-control study. *BMJ*. 1998 Dec 5;317(7172):1549-53.

19. Kurinczuk JJ, White-Koning M, Badawi N. Epidemiology of neonatal encephalopathy and hypoxic-ischaemic encephalopathy. Elsevier; 2010. p. 329-38.
20. Feather-Schussler DN, Ferguson TS. A Battery of Motor Tests in a Neonatal Mouse Model of Cerebral Palsy. *J Vis Exp*. 2016 Nov 3(117):e53569-e69.
21. Behrman RE, Butler AS. Mortality and acute complications in preterm infants. Preterm birth: causes, consequences & prevention. 2006.
22. Aziz NM, Guedj F, Pennings JLA, Olmos-Serrano JL, Siegel A, Haydar TF, et al. Lifespan analysis of brain development, gene expression and behavioral phenotypes in the Ts1Cje, Ts65Dn and Dp(16)1/Yey mouse models of Down syndrome. *Dis Model Mech*. 2018 Jun 12;11(6).
23. Baud O, Daire JL, Dalmaz Y, Fontaine RH, Krueger RC, Sebag G, et al. Gestational hypoxia induces white matter damage in neonatal rats: a new model of periventricular leukomalacia. *Brain Pathol*. 2004 Jan;14(1):1-10.
24. Mallard C, Vexler ZS. Modeling ischemia in the immature brain: How translational are animal models? 2015.
25. Kubo KI, Deguchi K, Nagai T, Ito Y, Yoshida K, Endo T, et al. Association of impaired neuronal migration with cognitive deficits in extremely preterm infants. *JCI Insight*. 2017 May 18;2(10).
26. Howell KR, Pillai A. Effects of prenatal hypoxia on schizophrenia-related phenotypes in heterozygous reeler mice: a gene x environment interaction study. *Eur Neuropsychopharmacol*. 2014 Aug;24(8):1324-36.
27. Howell KR, Pillai A. Long-Term Effects of Prenatal Hypoxia on Schizophrenia-Like Phenotype in Heterozygous Reeler Mice. *Mol Neurobiol*. 2016 Jul;53(5):3267-76.
28. McClendon E, Shaver DC, Degener-O'Brien K, Gong X, Nguyen T, Hoerder-Suabedissen A, et al. Transient Hypoxemia Chronically Disrupts Maturation of Preterm Fetal Ovine Subplate Neuron Arborization and Activity. *J Neurosci*. 2017 Dec 6;37(49):11912-29.
29. McClendon E, Wang K, Degener-O'Brien K, Hagen MW, Gong X, Nguyen T, et al. Transient Hypoxemia Disrupts Anatomical and Functional Maturation of Preterm Fetal Ovine CA1 Pyramidal Neurons. *J Neurosci*. 2019 Oct 2;39(40):7853-71.
30. Deacon RM. Assessing nest building in mice. *Nat Protoc*. 2006;1(3):1117-9.
31. Huang H, Zhang J, Wakana S, Zhang W, Ren T, Richards LJ, et al. White and gray matter development in human fetal, newborn and pediatric brains. *Neuroimage*. 2006 Oct 15;33(1):27-38.
32. Huang H, Yamamoto A, Hossain MA, Younes L, Mori S. Quantitative cortical mapping of fractional anisotropy in developing rat brains. *J Neurosci*. 2008 Feb 6;28(6):1427-33.
33. Huang H, Xue R, Zhang J, Ren T, Richards LJ, Yarowsky P, et al. Anatomical characterization of human fetal brain development with diffusion tensor magnetic resonance imaging. *J Neurosci*. 2009 Apr 1;29(13):4263-73.
34. Jiang H, van Zijl PC, Kim J, Pearlson GD, Mori S. DtiStudio: resource program for diffusion tensor computation and fiber bundle tracking. *Comput Methods Programs Biomed*. 2006 Feb;81(2):106-16.
35. Paxinos G, Franklin KBJ. Paxinos and Franklin's the Mouse Brain in Stereotaxic Coordinates. 2001.
36. Deacon RM. Digging and marble burying in mice: simple methods for in vivo identification of biological impacts. *Nat Protoc*. 2006;1(1):122-4.
37. Vorhees CV, Williams MT. Morris water maze: procedures for assessing spatial and related forms of learning and memory. *Nat Protoc*. 2006;1(2):848-58.
38. Witkin JM. Animal Models of Obsessive-Compulsive Disorder. Hoboken, NJ, USA: John Wiley & Sons, Inc.; 2008. p. 9.30.1-9.30.9.

39. Yang M, Silverman JL, Crawley JN. Automated three-chambered social approach task for mice. *Curr Protoc Neurosci*. 2011 Jul;Chapter 8:Unit 8 26.
40. Rothwell PE, Fuccillo MV, Maxeiner S, Hayton SJ, Gokce O, Lim BK, et al. Autism-associated neuroligin-3 mutations commonly impair striatal circuits to boost repetitive behaviors. *Cell*. 2014 Jul 3;158(1):198-212.
41. Simonet JC, Sunnen CN, Wu J, Golden JA, Marsh ED. Conditional Loss of Arx From the Developing Dorsal Telencephalon Results in Behavioral Phenotypes Resembling Mild Human ARX Mutations. *Cereb Cortex*. 2015 Sep;25(9):2939-50.
42. Tucker LB, McCabe JT. Behavior of Male and Female C57BL/6J Mice Is More Consistent with Repeated Trials in the Elevated Zero Maze than in the Elevated Plus Maze. *Front Behav Neurosci*. 2017;11:13.
43. Kadiyala SB, Papandrea D, Herron BJ, Ferland RJ. Segregation of seizure traits in C57 black mouse substrains using the repeated-flurothyl model. *PLoS One*. 2014;9(3):e90506.
44. Ferland RJ. The Repeated Flurothyl Seizure Model in Mice. *Bio Protoc*. 2017 Jun 5;7(11).
45. Halekoh U, Højsgaard S, Yan J. TheRPackagegeepackfor Generalized Estimating Equations. *Journal of Statistical Software*. 2006;15(2):1-11.
46. Bates D, Mächler M, Bolker B, Walker S. Fitting Linear Mixed-Effects Models Usinglme4. *Journal of Statistical Software*. 2015;67(1).
47. Demarest TG, Schuh RA, Waddell J, McKenna MC, Fiskum G. Sex-dependent mitochondrial respiratory impairment and oxidative stress in a rat model of neonatal hypoxic-ischemic encephalopathy. *J Neurochem*. 2016 Jun;137(5):714-29.
48. Aravamuthan BR, Gandham S, Young AB, Rutkove SB. Sex may influence motor phenotype in a novel rodent model of cerebral palsy. *Neurobiol Dis*. 2020 Feb;134:104711.
49. Semenza GL. Oxygen sensing, hypoxia-inducible factors, and disease pathophysiology. *Annu Rev Pathol*. 2014;9(1):47-71.
50. Trollmann R, Strasser K, Keller S, Antoniou X, Grenacher B, Ogunshola OO, et al. Placental HIFs as markers of cerebral hypoxic distress in fetal mice. *Am J Physiol Regul Integr Comp Physiol*. 2008 Dec;295(6):R1973-81.
51. Nakajima W, Ishida A, Lange MS, Gabrielson KL, Wilson MA, Martin LJ, et al. Apoptosis has a prolonged role in the neurodegeneration after hypoxic ischemia in the newborn rat. *J Neurosci*. 2000 Nov 1;20(21):7994-8004.
52. Belet N, Belet U, Incesu L, Uysal S, Ozinal S, Keskin T, et al. Hypoxic-ischemic encephalopathy: correlation of serial MRI and outcome. *Pediatr Neurol*. 2004 Oct;31(4):267-74.
53. Brooks SP, Dunnett SB. Tests to assess motor phenotype in mice: A user's guide. 2009.
54. Jaramillo TC, Speed HE, Xuan Z, Reimers JM, Escamilla CO, Weaver TP, et al. Novel Shank3 mutant exhibits behaviors with face validity for autism and altered striatal and hippocampal function. *Autism Res*. 2017 Jan;10(1):42-65.
55. Drapeau E, Riad M, Kajiwarra Y, Buxbaum JD. Behavioral Phenotyping of an Improved Mouse Model of Phelan-McDermid Syndrome with a Complete Deletion of the Shank3 Gene. *eNeuro*. 2018 May-Jun;5(3).
56. Cryan JF, Holmes A. Model organisms: The ascent of mouse: Advances in modelling human depression and anxiety. 2005.
57. Van Handel M, Swaab H, De Vries LS, Jongmans MJ. Long-term cognitive and behavioral consequences of neonatal encephalopathy following perinatal asphyxia: A review. 2007.
58. Shankaran S, Pappas A, McDonald SA, Vohr BR, Hintz SR, Yolton K, et al. Childhood outcomes after hypothermia for neonatal encephalopathy. *N Engl J Med*. 2012 May 31;366(22):2085-92.

59. van Handel M, Swaab H, de Vries LS, Jongmans MJ. Behavioral outcome in children with a history of neonatal encephalopathy following perinatal asphyxia. *J Pediatr Psychol*. 2010 Apr;35(3):286-95.
60. Barnett A, Mercuri E, Rutherford M, Haataja L, Frisone MF, Henderson S, et al. Neurological and perceptual-motor outcome at 5 - 6 years of age in children with neonatal encephalopathy: relationship with neonatal brain MRI. *Neuropediatrics*. 2002 Oct;33(5):242-8.
61. Annink KV, de Vries LS, Groenendaal F, van den Heuvel MP, van Haren NEM, Swaab H, et al. The long-term effect of perinatal asphyxia on hippocampal volumes. *Pediatr Res*. 2019 Jan;85(1):43-49.
62. Tomita S, Ueno M, Sakamoto M, Kitahama Y, Ueki M, Maekawa N, et al. Defective brain development in mice lacking the Hif-1alpha gene in neural cells. *Mol Cell Biol*. 2003 Oct;23(19):6739-49.
63. Perlman JM. Pathogenesis of hypoxic-ischemic brain injury. *Journal of Perinatology*. 2007;27(S1):S39-S46.
64. Peebles PJ, Duello TM, Eickhoff JC, McAdams RM. Antenatal and intrapartum risk factors for neonatal hypoxic ischemic encephalopathy. *J Perinatol*. 2020 Jan;40(1):63-69.
65. Stowe AM, Altay T, Freie AB, Gidday JM. Repetitive hypoxia extends endogenous neurovascular protection for stroke. *Ann Neurol*. 2011 Jun;69(6):975-85.
66. Jensen FE, Applegate CD, Holtzman D, Belin TR, Burchfiel JL. Epileptogenic effect of hypoxia in the immature rodent brain. *Ann Neurol*. 1991 Jun;29(6):629-37.
67. Gopagondanahalli KR, Li J, Fahey MC, Hunt RW, Jenkin G, Miller SL, et al. Preterm hypoxic-ischemic encephalopathy. *Frontiers Media SA*; 2016. p. 114-14.
68. Salmaso N, Jablonska B, Scafidi J, Vaccarino FM, Gallo V. Neurobiology of premature brain injury. *Nat Neurosci*. 2014 Mar;17(3):341-6.
69. Glass HC, Hong KJ, Rogers EE, Jeremy RJ, Bonifacio SL, Sullivan JE, et al. Risk factors for epilepsy in children with neonatal encephalopathy. *Pediatr Res*. 2011 Nov;70(5):535-40.
70. Smith AL, Alexander M, Rosenkrantz TS, Sadek ML, Fitch RH. Sex differences in behavioral outcome following neonatal hypoxia ischemia: insights from a clinical meta-analysis and a rodent model of induced hypoxic ischemic brain injury. *Exp Neurol*. 2014 Apr;254:54-67.
71. Hill CA, Fitch RH. Sex differences in mechanisms and outcome of neonatal hypoxia-ischemia in rodent models: Implications for sex-specific neuroprotection in clinical neonatal practice. 2012.
72. Charriaut-Marlangue C, Besson VC, Baud O. Sexually dimorphic outcomes after neonatal stroke and hypoxia-ischemia. *MDPI AG*; 2018.
73. Baron-Cohen S, Knickmeyer RC, Belmonte MK. Sex differences in the brain: implications for explaining autism. *Science*. 2005 Nov 4;310(5749):819-23.

Figure Legends

Fig. 1: Prenatal hypoxia paradigm induces a canonical HIF1 α response consistent with hypoxic insult in the fetal brains.

(A) Representative immunoblot of HIF1 α protein in fetal brains after indicated time of prenatal hypoxia. (B) HIF1 α protein quantification shown. Statistics by One-Way ANOVA with Dunnett's multiple comparison test for statistical significance. (C) Vegfa mRNA levels after time of prenatal hypoxia. Points shown in graphs are from individual fetal brains. Nested One-Way ANOVA with Dunnett's multiple comparison test for statistical significance.

Fig. 2: Maternal dams make normal nests and there is no early difference in litter health.

(A) Cumulative distance over time of pregnant dams during the first 90 minutes the mice were in chamber. Area under the curve is shaded and the dashed line around each condition represents SEM of respective condition. Dashed black line is where mice reach 10% O₂. Statistics shown for the first 20 minutes of chamber exposure and then for 1 hour after hypoxic mice reached goal oxygen level. (B) Scoring of maternal nestlets the morning after normoxia or hypoxia. Points represent individual dams that were assessed. (C) Litter size at birth and (D) gestational age at birth for indicated individual litters were assessed. Welch's t-test used for (A-D). (E) Percent survival of offspring. Error bars represent standard error at that time point. Log-rank test used for statistics with normoxia (solid black line) n = 19; hypoxia (dashed blue line) n = 28.

Fig. 3: Prenatal hypoxia does not increase cell death in the fetal brain. (A) Representative image of pyknotic nuclei. Scale bar represents 200 μ M (B-D) Number of pyknotic nuclei in the cortex, basal ganglia, and white matter, reported as average seen in 10 separate high powered fields. Welch's t-test was used to determine statistical significance.

Fig. 4: Prenatal hypoxia does not result in long-term gross neuroanatomical damage (A) Axial images of adult female brain MRI (averaged b0 map) of indicated conditions from individual mice. (B) Quantification of ventricular size in the setting of normoxia and hypoxia. Hypoxic animals from (A) represented by indicated symbols in (B). (C) Mid-sagittal image demonstrating the areas that were quantified, the anterior cingulate cortex (light blue line) the genu of the corpus callosum (orange circle), and the splenium of the corpus callosum (pink circle). (D) Quantification of cortical thickness at the anterior cingulate. (E & F) Quantification of fractional anisotropy in mid-sagittal

areas of the genu and splenium of the corpus callosum respectively. Statistics as outlined in the methods. Points represent individual mice.

Fig. 5: Prenatal hypoxia leads to functional deficits in adult mice. (A) Flurothyl seizure threshold study demonstrating time to first GTC. (B & C) Data from Grip strength. (B) Forelimbs and (C) hindlimbs force. (E) Number of marbles buried. (F)) Change in nestlet weight in short term nestlet test. Statistics as outlined in the methods. Points represent individual mice.

Fig. 6. Sex-dichotomous behaviour differences after prenatal hypoxia. (A) Time spent in open arms in Elevated zero maze. (B) Total time animals spent in the center of Open field. (A-D) Percent time in each individual chamber during stages of social interaction study. (A-B) Data from habituation stage from males and females. (C-D) Data from novel mouse/object stage from males and female. (E-H) Percent time mice spent sniffing at the plastic clear tube. Statistics as outlined in the methods. Points represent individual mice.

Fig. 7: Prenatal hypoxia does not lead to deficits in learning or memory. (A) Speed at fall on Rotarod. (B-C) Data from Morris Water Maze. (B)) Latency time to platform in place trials. (C) One-hour probe trial. (D) Twenty-four hour probe trial. Statistics performed as detailed in methods. Each point represents a single animal.

Figure 1

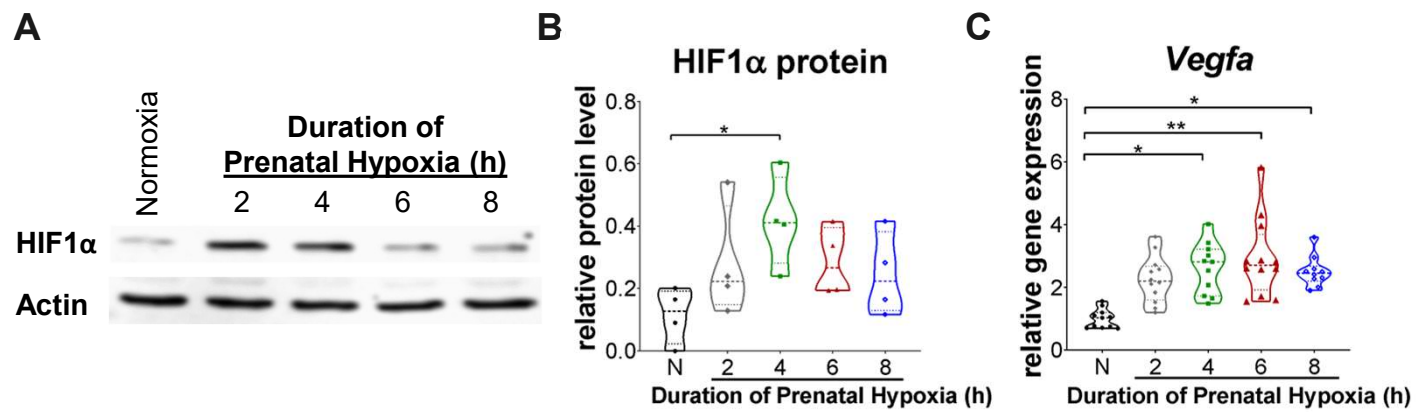


Figure 2

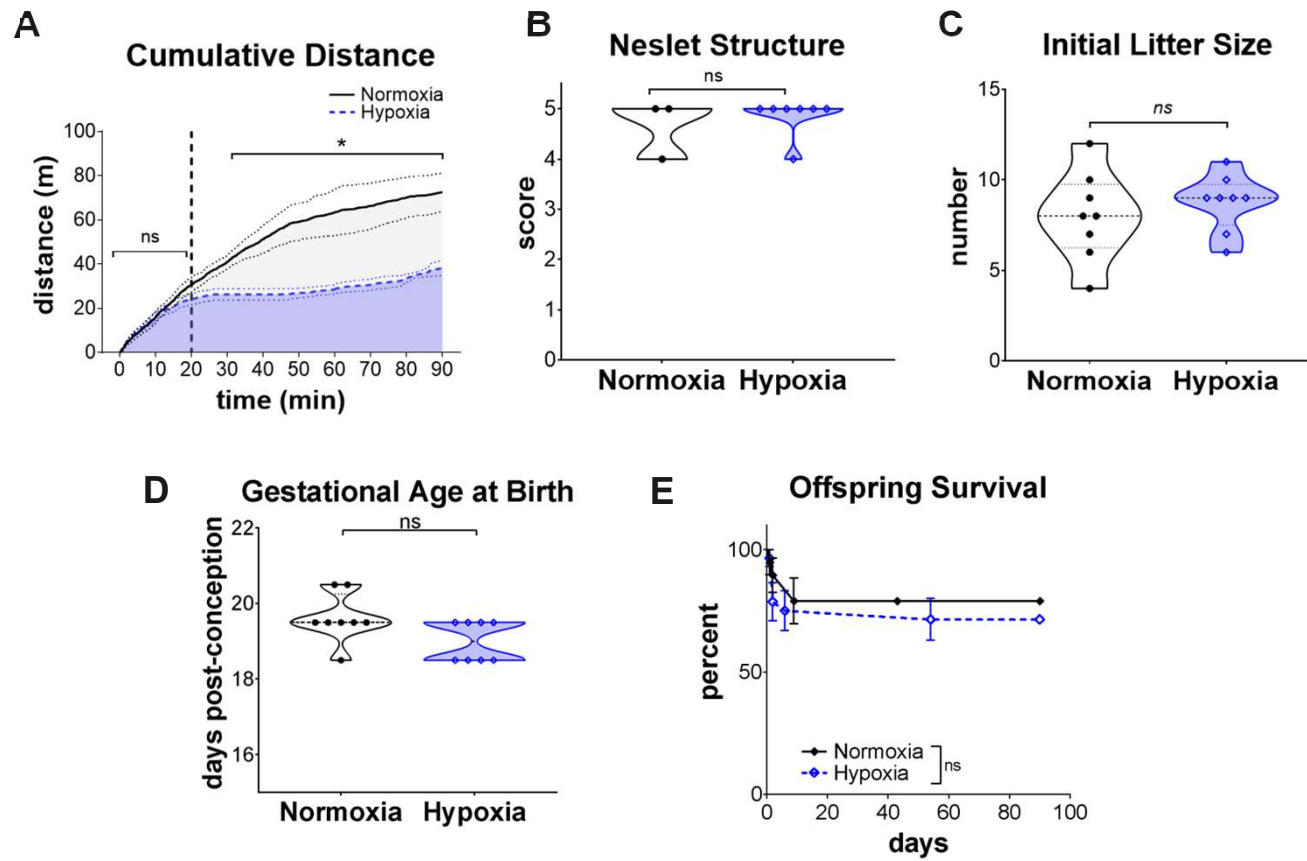


Figure 3

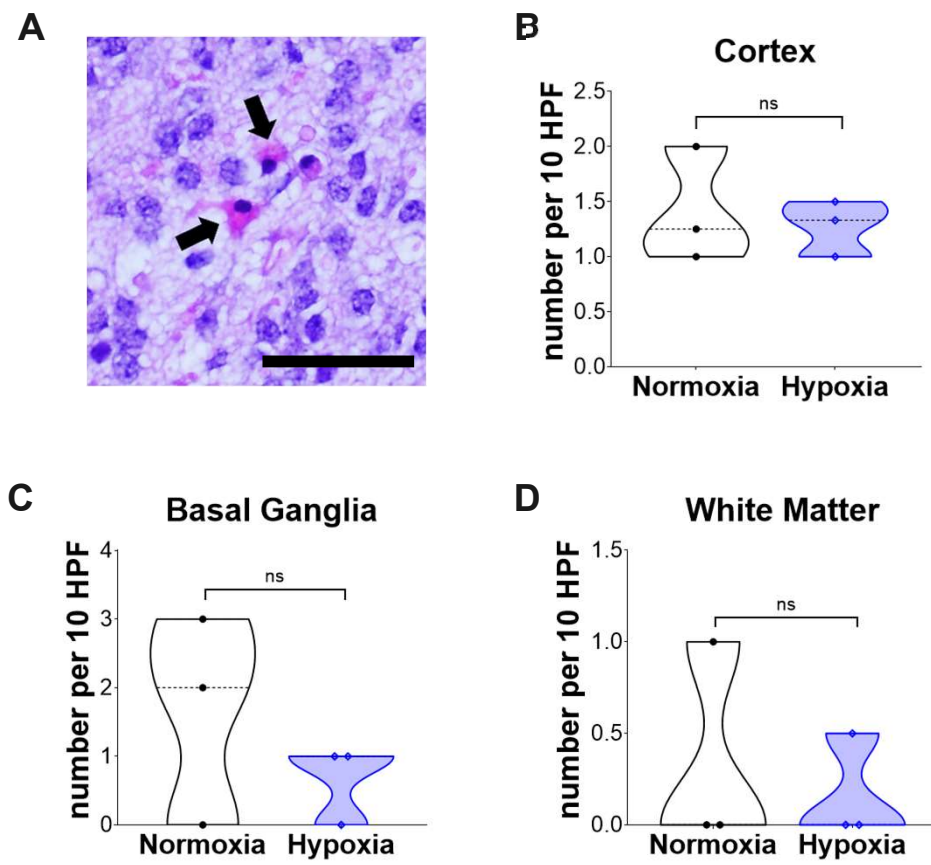


Figure 4

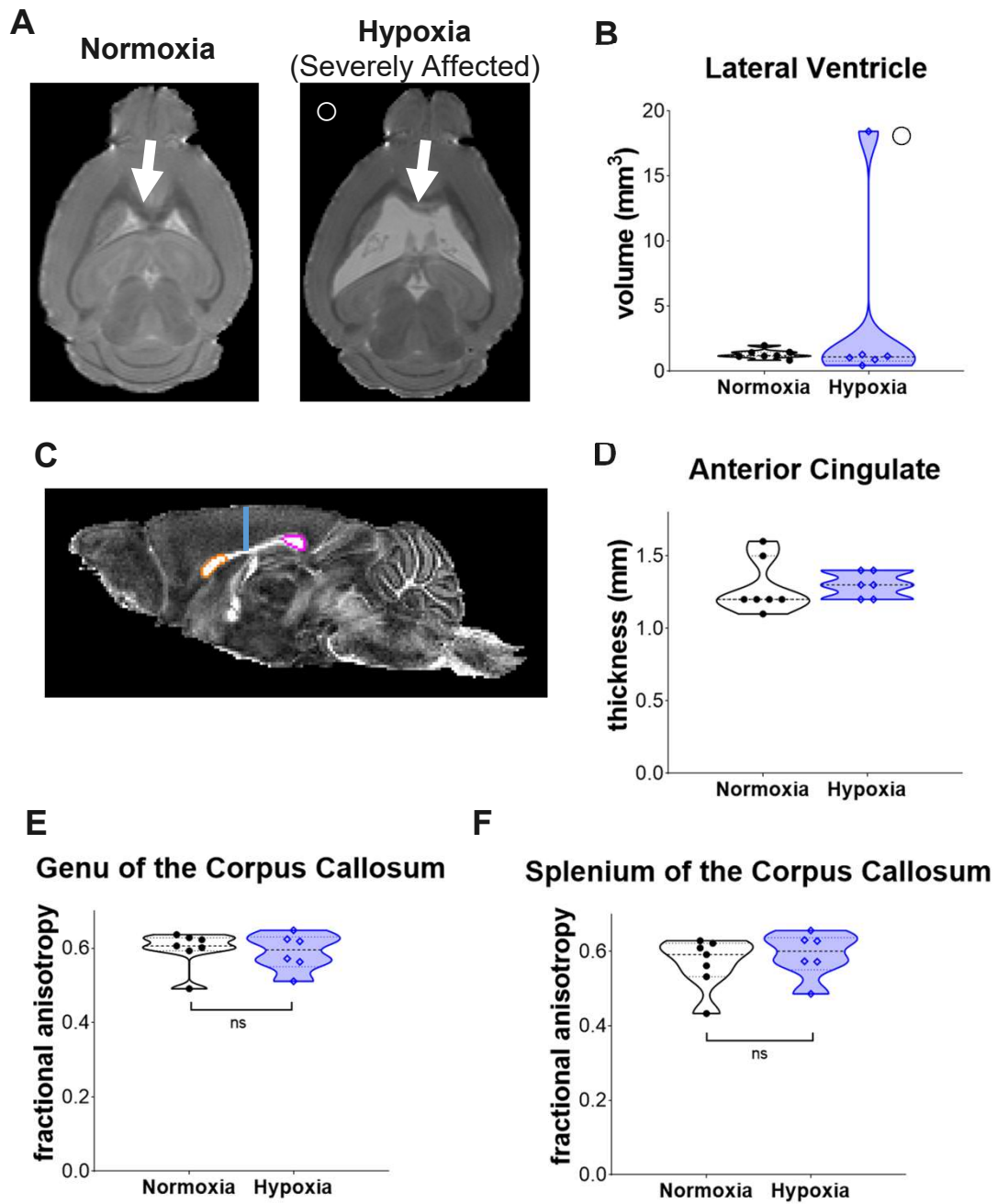


Figure 5

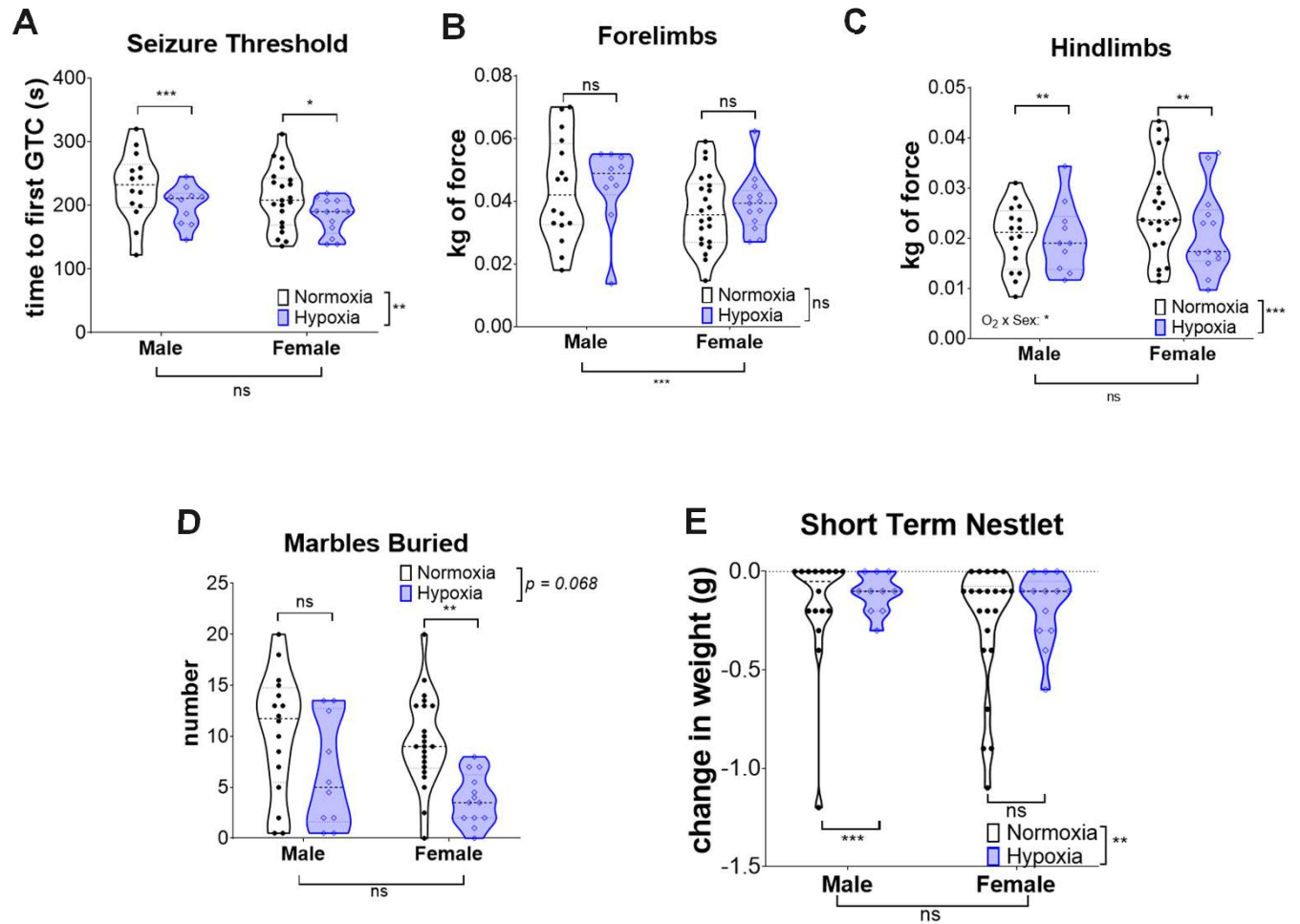


Figure 6

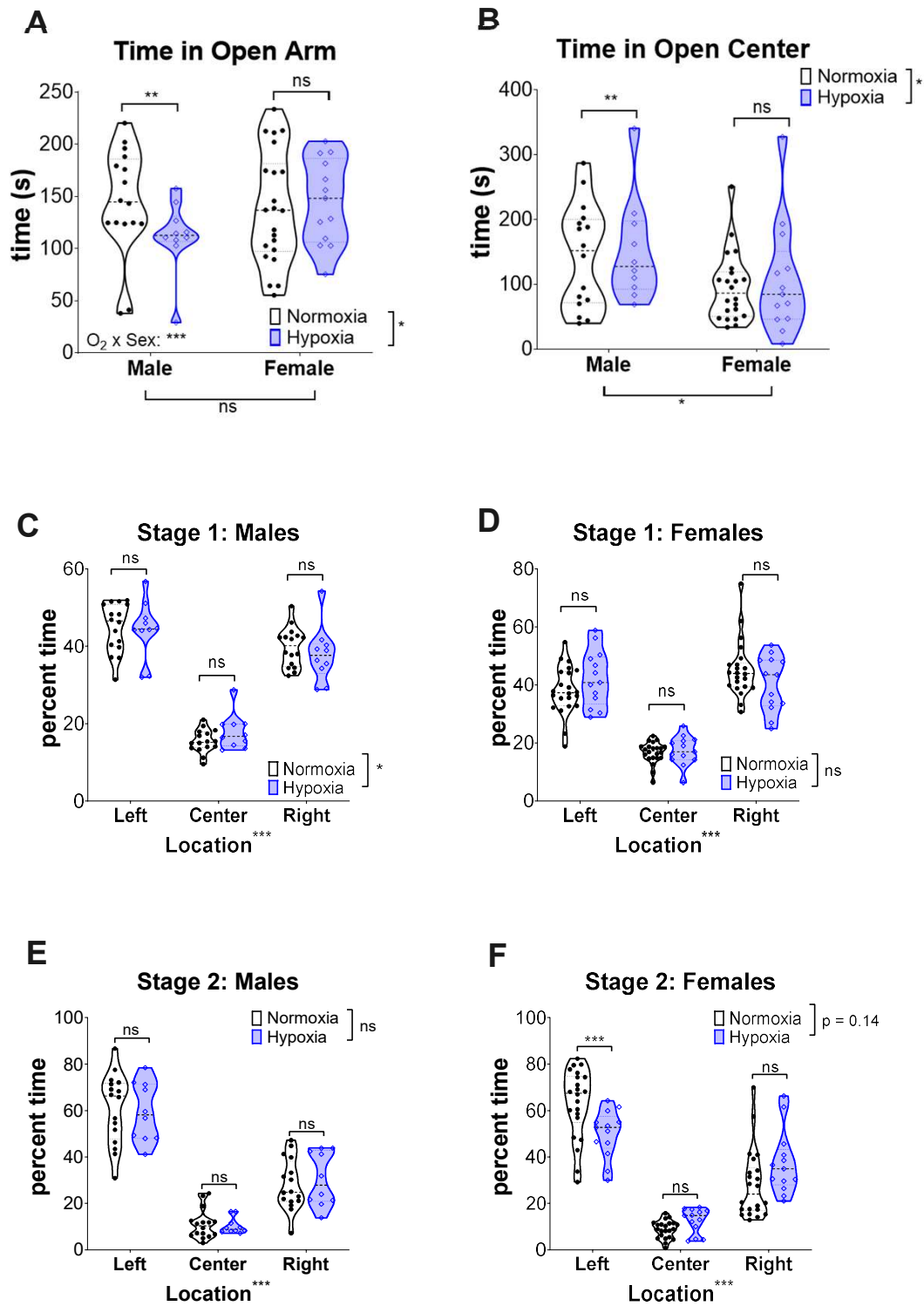


Figure 7

